REPORT DOCUMENTATION PAGE

Form Approved
OMB No. 074-0188

Public reporting burden for this collection of information is estimated to average 1 hour per response, including the time for reviewing instructions, searching existing data sources, gathering and maintaining the data needed, and completing and reviewing this collection of information. Send comments regarding this burden estimate or any other aspect of this collection of information, including suggestions for reducing this burden to Washington Headquarters Services, Directorate for Information Operations and Reports, 1215 Jefferson Davis Highway, Suite 1204, Arlington, VA 22202-4302, and to the Office of Management and Budget, Paperwork Reduction Project (0704-0188), Washington, DC 20503

1. AGENCY USE ONLY (Leave blank)	2. REPORT DATE	3. REPORT TYPE AND DATES COVERED
	18 March 1994	Technical report, 1994

4. TITLE AND SUBTITLE
Ultraviolet and Radical Oxidation of Airborne VOC's

5. FUNDING NUMBERS
N/A

6. AUTHOR(S)
Robert Jennings Heinsohn, Timothy A. Spaeder, Maria T. Albano, John P. Schmelzle and Robert O. Fetter

7. PERFORMING ORGANIZATION NAME(S) AND ADDRESS(ES)
140 Reber Building of Mechanical Engineering
The Pennsylvania State University
University Park, PA 16802

8. PERFORMING ORGANIZATION REPORT NUMBER
N/A

9. SPONSORING / MONITORING AGENCY NAME(S) AND ADDRESS(ES)
SERDP
901 North Stuart St. Suite 303
Arlington, VA 22203

10. SPONSORING / MONITORING AGENCY REPORT NUMBER
N/A

11. SUPPLEMENTARY NOTES
Presented at the First International Conference on Advanced Oxidation Technologies for Water and Air Remediation, London, Ontario, Canada, June 1994. This work was supported in part by SERDP. The United States Government has a royalty-free license throughout the world in all copyrightable material contained herein. All other rights are reserved by the copyright owner.

12a. DISTRIBUTION / AVAILABILITY STATEMENT
Approved for public release: distribution is unlimited

12b. DISTRIBUTION CODE
A

13. ABSTRACT ***(Maximum 200 Words)***

Airborne VOC's reactions initiated by UV radiation at selected wave lengths from 185 to 308 nm have been studied. A simplified chemical kinetic mechanism is proposed incorporating photolysis and radical reactions. The concentration of HCHO and CH_3OH were predicted as a function of time, radiation wave length, actinic flux and initial ozone concentration. The gas velocity and HCHO concentration were predicted in a gas stream flowing over a UV bulb. Experiments were conducted in which ethanol vapor and air were irradiated by low-pressure mercury bulbs. Ethanol disappeared in an overall first-order manner and an intermediate species, believed to be acetaldehyde, appeared and then disappeared.

14. SUBJECT TERMS
airborne VOC's, UV radiation, photolysis, radical oxidation, SERDP

15. NUMBER OF PAGES
24

16. PRICE CODE
N/A

17. SECURITY CLASSIFICATION OF REPORT	18. SECURITY CLASSIFICATION OF THIS PAGE	19. SECURITY CLASSIFICATION OF ABSTRACT	20. LIMITATION OF ABSTRACT
unclass	unclass	unclass	UL

NSN 7540-01-280-5500

Standard Form 298 (Rev. 2-89)
Prescribed by ANSI Std. Z39-18
298-102

DTIC QUALITY INSPECTED 19980817 164

Reproduced From
Best Available Copy

49 - 1994

ULTRAVIOLET AND RADICAL OXIDATION OF AIRBORNE VOC'S

Robert Jennings Heinsohn *
Timothy A. Spaeder **
Maria T. Albano ***
John P. Schmelzle ***
Robert O. Fetter *****

* Mechanical Engineering
** Environmental Engineering
*** Environmental Pollution Control Program
**** Lieutenant, U. S. Navy CEC

*140 Reber Building of Mechanical Engineering, The Pennsylvania State University, University Park, PA, 16802 (814-863-1198, FAX 814-863-4848)

18 March 1994

ABSTRACT

Airborne VOC 's reactions initiated by UV radiation at selected wave lengths from 185 to 308 nm have been studied. A simplified chemical kinetic mechanism is proposed incorporating photolysis and radical reactions. The concentration of HCHO and CH_3OH were predicted as a function of time, radiation wave length, actinic flux and initial ozone concentration. The gas velocity and HCHO concentration were predicted in a gas stream flowing over a UV bulb. Experiments were conducted in which ethanol vapor and air were irradiated by low-pressure mercury bulbs. Ethanol disappeared in an overall first-order manner and an intermediate species, believed to be acetaldehyde, appeared and then disappeared.

ULTRAVIOLET AND RADICAL OXIDATION OF AIRBORNE VOC'S

Pollution control systems using ultraviolet (UV) radiation have received considerable attention in recent years. The EPA's SITE program (1,2) evaluated concepts using UV to oxidize organic compounds in water and air. Since oxidation occurs at STP, the nitrogen oxides associated with high-temperature thermal destruction are not generated. There is considerable evidence (3-8) that the generation of hydroxyl radicals (OH) is enhanced when surfaces coated with titania (TiO_2) are irradiated. To design, predict and optimize the performance of UV reactors, engineers need relationships that integrate the equations of chemical kinetics with the equations of fluid mechanics, i.e. conservation of mass, momentum and energy. Engineers presently lack these integrated relationships. This paper reports studies of airborne VOC's subjected to UV radiation in the absence of titania with the overall objective of providing insight for the design of photolytic reactors. Specifically , the paper

- proposes a simplified chemical kinetic mechanism for methanol (CH_3OH) and formaldehyde (HCHO) subjected to UV radiation,
- predicts the velocities and [HCHO] in air flowing over a UV lamp,
- presents the results of experiments of ethanol (C_2H_5OH) in air flowing over UV bulbs.

PREVIOUS STUDIES

Martinez et. al. (9) studied the near-UV absorption spectra ($\lambda < 200$ nm) of several aliphatic aldehydes and ketones and found that,

- the photolysis of acetaldehyde was slow compared with reactions with OH,
- photolysis reactions with OH proceed at comparable rates for acetone and larger aldehydes,
- depending on the quantum yields, the photo-dissociation of larger ketones may be more important than reactions with OH.

Using a 2756-watt pulsed xenon flash lamp ($\lambda_{max} = 230nm$) and a well mixed reactor, Johnson et. al. (10) proposed photo-induced chain reaction mechanisms and first-order, photo-induced decay coefficients for a variety of hallogenated hydrocarbons. Anastasi et. al. (11) described reactions involving alkenes, alcohols and ethers. They proposed a chemical amplification system in which HO_2 reacts with NO to form NO_2 and OH, and then OH reacts with chain-carrying agents to reform peroxy radicals to restart the chain.

Part I - CHEMICAL KINETICS

To design a UV reactor, engineers need to model the reactions in the flow of airborne VOC's passing around a selected geometrical configuration of bulbs. Decisions need to be made regarding the bulb configuration and whether it is advantageous to inject O_3, H_2O_2 or other materials into (or upstream) of a region containing UV bulbs. A modeling prerequisite, is a description of the chemical kinetic mechanism initiated by UV radiation. Solving the equations of fluid mechanics is straight forward but writing the equations of chemical kinetics is difficult. Formulating such a kinetic mechanism begins by identifying all the reactions that may occur and then eliminating reactions of minimal numerical importance.

In this study only process gas streams produced by industrial processes occurring at STP (surface cleaning and coating, solvent venting, etc.) will be considered. Ignored are process gas streams produced by high-temperature processes. Consequently, the airborne VOC's are primarily aliphatic and aromatic hydrocarbons and alcohols in air containing water vapor and nitrogen oxides typically found in the indoor and outdoor air at STP. Typically, gas volumetric flow rates are several hundred cubic meters per second and gas velocities are of the order of tens of m/s. The VOC's chosen for study were HCHO and CH_3OH. While these species are not typically found in industrial gas streams, they were chosen because HCHO is photolytic and because the chemical kinetic mechanism for these species is well known. In Part I the gas mixture was assumed to be stationary and contained in a vessel whose walls do not reflect or generate radiation, adsorb species nor support chemical reactions, i.e. a wall-less reactor. The radiation actinic flux (J, photons/m^2s) was assumed to be constant.

Reactions included in the model were drawn from the literature on urban photochemistry (11-24). Nitrogen oxides larger than NO_2 were ignored. Shown in Table I are the sources of the UV radiation and initial concentrations for five cases chosen for study. Shown in Table II are the radical reactions and rate constants drawn from the literature (11-24).

The actinic flux is related to the wave length,

$$J = \left(\frac{P_\lambda}{A}\right)\left(\frac{\lambda}{hc}\right) \qquad (1)$$

where,

λ = radiation wave length
P_λ / A = radiation power at wave length λ per unit area,
h, c = Planck's constant and speed of light
E_λ = energy of photons at wave length λ

Photolytic rate constants are related to the actinic flux,

$$k = \int_{\lambda_1}^{\lambda_2} \sigma(T,\lambda)\varphi(T,\lambda)I(\lambda)d\lambda \qquad (2)$$

or in finite form,

$$k = \sum_{\lambda_1}^{\lambda_2} \sigma(\lambda_i,T)\varphi(\lambda_i,T)J(\lambda_i) \qquad (3)$$

where,

- $\sigma(\lambda,T)$ = absorption cross section of a specific molecule at temperature T and wavelength λ (cm^2)
- $\varphi(\lambda,T)$ = primary quantum yield, probability that the molecule will follow one of a number of prescribed chemical kinetic pathways
- $I(\lambda)$ = irradiance of incident UV radiation
- $J(\lambda) = I(\lambda)d\lambda$

The photolytic rate constants for the five cases are shown in Table III and were computed from values φ and σ taken from the literature (25-27).

RESULTS

A set of 20 simultaneous ordinary differential equations was written and solved for the radical and photolytic reactions in Tables II and III. The concentration of each species was computed as a function of time using a fourth-order Runge Kutta numerical technique. Figures 1 and 2 show [HCHO] and [CH_3OH] versus time.

Effect of initial ozone concentration for low-intensity radiation (Cases 1 & 2)

For low-pressure mercury lamps, there is minimal (0.2%) oxidation of HCHO in ambient air after several seconds of irradiation (Case 1) , whereas there is substantial oxidation when $[O_3]_0$ is 1000 PPM (Case 2). Graphs of predicted values of [O_3], [H_2O_2], [OH], [HO_2], [O^1D] and [O^3P] indicate that rapid changes in concentration occur during a "startup period" ($0 < t < 0.5$ s) and that uniform change occurs thereafter. The steadiness of change after startup enables an order of magnitude analysis to be performed to eliminate reactions in Table II that have little numerical significance. The resulting simplified kinetic mechanism is shown in Figs 3 and 4. For simplicity, reactions involving nitrogen oxides have been omitted from Fig 3 because they represent parallel and competing paths that consume OH and only minimally affect VOC oxidation. Since the process gas streams under study are not produced by an exothermic process, large initial concentrations of nitrogen oxides are not expected. Thus unlike

atmospheric photochemical processes in which nitrogen oxides play a major role, their role is less significant in process gas streams containing VOC concentrations in thousands of parts per million.

The simplified reaction scheme consists the direct photolysis of HCHO, but more importantly, pathways for reactions between OH and HCHO and CH_3OH. Hydroxyl radicals are generated directly by the photolysis of water vapor (P7B) and by two overlapping pathways, i.e. (a) ozone loop and (b) HO_2 loop

The Ozone Loop consists of reactions in which ozone reacts with H to form OH (R19) and reactions of ozone with OH to form HO_2 (R1). Ozone photolysis may occur (P3A) to form O^1D which either reacts with H_2O to form two OH (R36) or reacts with N_2 (R30) or O_2 (R38) to form O^3P which reconstitutes ozone (R31).

The HO_2Loop generates the hydroperoxyl radical in several ways. It is generated by O_2 reactions with H (R18) or HCO (R9), or reactions between OH and ozone (R1) and H_2O_2 (R13). Once formed, HO_2 reacts with O_2 (R2) to form OH or with itself (R20) to form H_2O_2. Hydrogen peroxide either reacts with UV to form two OH (P5A), or reacts with OH (R13) to form HO_2 which ultimately produces OH. In summary, HO_2 is an intermediate radical that is generated and consumed at the expense of ozone and hydrocarbon radicals. Ultimately HO_2 leads to the generation of OH.

To use the simplified reaction scheme users need to solve simultaneously 9 ordinary differential equations simultaneously (Fig 4).

It is concluded that the most important species in the simplified scheme is ozone. With the exception of arid regions, ordinary air contains copious quantities of water vapor and there are ample quantities of H_2O for reactions P7B and R36 to produce OH radicals. For this reason, the production of OH is primarily dependent on the supply of ozone. It is not possible to simultaneously generate and use ozone since it is consumed as fast as it is generated. Since the amount of ozone in ordinary air is small, engineers will find it necessary to enrich air with ozone prior to its introduction into the photolytic reactor.

Effect of UV wavelength on VOC oxidation in ordinary air (Cases 3,4 and 5)

Cases 3-5 in Figs 1 and 2 show that when the actinic flux is large oxidation is achieved for several UV wavelengths even when the initial ozone concentration is small. Unfortunately such high-energy radiation may be impossible to generate economically for the large volumetric flow rates typically encountered in process gas streams. Excimer lasers consume considerable energy and it is unclear whether more efficient sources will be available in the near future. Thus while high-energy UV sources eliminate the need to enrich the air with ozone, it is not clear

whether efficient sources of high-energy UV radiation are or will be available in the near future. Enriching air with several hundred PPM of ozone is presently possible at modest cost. Thus it will be more economical to enrich the process gas stream with ozone than to use ordinary air and high-energy UV sources.

Oxidation of higher-order VOC's

If the process gas stream contains higher-order VOC's, the initial attack on the VOC's is more complicated. Reactions need to be added to the beginning of Fig 4 that account for the initial attack of OH and O^1D on higher-order hydrocarbons to produce complex hydrocarbon radicals and HCHO. Once this is done, the remaining reactions will then be similar to those in Fig 4. Alternatively, higher-order hydrocarbons can be modeled using the carbon bond model (28,29) and Cal Tech models (13,14,30) without needing detailed knowledge of the explicit steps in the kinetic mechanism.

From studies in which the inlet concentration and UV wavelengths were varied, the following conclusions were drawn.

- Large actinic flux produce rapid oxidation of VOC's over a wide range of UV wavelengths.
- Rapid oxidation of VOC's can not be achieved with modest actinic fluxes unless the initial ozone concentration is considerably greater than that found in typical urban air. At modest actinic flux, it is unwise to attempt to generate ozone and oxidize VOC's simultaneously. Ozone should be generated independently and introduced at the inlet of the photolytic reactor.

Part II - PHOTOLYSIS OF HCHO IN A UNIFORM FLOW FIELD OVER A UV LAMP

To illustrate how the equations of chemical kinetics can be incorporated with the equations of fluid mechanics, consider only the photolysis of airborne HCHO streaming over a cylindrical UV bulb whose axis is perpendicular to the flow (Fig 5). For computational simplicity, the radical reactions in Table II were replaced by a single vigorous photolysis reactions (P1A and P1B). The actinic flux and hence the photolysis rate constant varied inversely with the radius from the bulb axis. The rate constant was equal to 0.35 s^{-1} at the bulb surface. Such a rate constant is nearly 10^4 larger than in cases 1 and 2 but comparable to cases 3, 4 and 5. The equations describing the velocity field are independent of the HCHO concentration field because the flow is isothermal and the HCHO concentration is sufficiently low so that the overall molar concentration does not change. Fluid flow is viscous and two dimensional. The two dimensional velocity field was predicted by a commercially available computational fluid dynamic computer program, FLUENT, (31). Figure 5 shows the predicted streamlines. The flow field is typical of turbulent flow over a cylinder and shows the wake region, and a recirculation eddy downstream of the lamp. Once the velocity field $\vec{U}(x,y)$ was

predicted, the differential equation for the conservation of mass was solved numerically to predict the concentration (C) of HCHO at arbitrary points (x ,y) in the flow domain.

$$-\vec{U} \bullet \nabla C + D\nabla^2 C + S = dC / dt \qquad (4)$$

The parameter D is the diffusion coefficient and S is the HCHO generation rate (P1A and P1B). The finite difference equation was developed using upwind differencing for the advection term and central differencing for the diffusion term. The equation was then solved for the formaldehyde concentration using the Gauss-Seidel method. An initial $[HCHO]_0$ of 50 PPM was used in the analysis.

Figure 6 shows steady state [HCHO] isopleths. Steep [HCHO] gradients exist in the boundary layer on the upstream of the bulb. Air with reduced [HCHO] is transported from the boundary layer at the 12 o'clock position on the bulb to mix with air in downstream side of the bulb. In the wake region, [HCHO] concentrations are low due in part to photolysis and in part to dilution of air with low [HCHO] transported from the upstream side of the bulb. Approximately five bulb diameters downstream of the bulb, the reactions have virtually ceased as evidenced by the constant values of [HCHO] along stream lines. Consequently,

- there is significant HCHO photolysis in the boundary layer around the bulb and little photolysis far upstream, above and below the bulb,
- there is little photolysis beyond five bulb diameters, downstream of the bulb.

Figure 6 shows that there is a large region above and below the bulb in which no reaction occurs. A useful measure of HCHO oxidation efficiency can be obtained by defining the HCHO oxidized in a stream tube whose width is equal to the diameter of the bulb (D_b). Such an efficiency will be called the "single-bulb" oxidation efficiency (η_b).

$$\eta_b = (\text{removed HCHO/entering HCHO})_{\text{stream tube of width } D_b}$$
$$= 1 - (C_{\text{avg outlet}}/C_{\text{inlet}})_{\text{stream tube of width } D_b} \qquad (5)$$

For the bulb shown in Fig 6, η_b was found to be 6.5%.

For a photolytic reactor containing an array (in-line or staggered) of n bulbs, the overall reactor oxidation efficiency (η_0) will be,

$$\eta_0 = 1 - (1 - \eta_b)^n \qquad (6)$$

Thus while single-bulb efficiencies may be modest, an array of bulbs can have a significant overall efficiency. For example, a photolytic reactor containing 20 bulbs in a row whose individual oxidation is described in Fig 6, would have an overall oxidation efficiency of 73.9%.

A reactor containing an array of UV bulbs is capable of oxidizing a significant fraction of airborne VOC's. The bulk of the reaction occurs in the bulb boundary layer and in the wake immediately behind the bulb. It is suggested that designers borrow concepts from the design of compact heat exchangers and pack bulbs in a dense array (in-line or staggered) approximately two bulb diameters between centers.

Part III - EXPERIMENTAL STUDIES

Ethanol vapor in air was irradiated by three, 40-watt, low-pressure mercury lamps inside the recirculating closed-loop apparatus shown in Fig 7. The bulbs were approximately 1.2 m long and 1 cm in diameter and aligned 3 cm between centers. The laser was omitted. A circulating fan (14.2 m^3/min.) produced an average gas velocity of 18.6 m/s parallel to the axis of the UV bulb. The gas was irradiated for a period of 0.08 s on each pass, a full pass required 0.275 s. The total length of the loop was 5.2 m and the internal volume was 0.065 m^3.

Reagent grade ethanol was injected into the air circulating in the test loop and allowed to vaporize. The initial ethanol mol fraction was 0.06. Gas samples were taken every minute for 20 minutes after irradiation and analyzed by an HP 5890 Series II gas chromatograph using a flame ionization detector. When irradiated, the logarithm of the [C_2H_5OH] decreased linearly with time (Fig 8) indicating an overall, first-order reaction. When adjusted for wall loss, the first-order rate constant was found to be of 1.76×10^{-5} s^{-1}. This value is consistent with the overall rate constants reported by Johnson et. al. (10) assuming overall rate constants are proportional to the input power to the UV lamps.

Chromatograms taken every minute over a 20-minute period, indicated that an intermediate species appeared simultaneously with the disappearance of ethanol. Based on the kinetic mechanism of ethanol oxidation (11) it is believed that the intermediate species is acetaldehyde. Acetaldehyde is known (9) to disappear by both photolysis and radical attack and was found to depend on the actinic flux.

Ethanol is not photolytic and hence its removal depends on the generation of OH and O_3. Of the radiation produced by the low-pressure mercury lamps only that portion at 185 nm is capable of producing O_3 (P4B). Once O_3 is formed, OH can be produced by the ozone and HO_2 loop in Part I. Table I shows that only 5% of the output radiant power from the low-pressure mercury lamp used in the experiment was at 185 nm. The overall conversion of input electrical power to radiation power is 40%, and of than only 5% is at 185 nm. Consequently

three, 40-watt lamps produces 2.4 watts of usable radiation at 185 nm. The ratio of electrical power to oxidize ethanol to the volumetric flow rate was 0.17 watts/m^3 /min.

CONCLUSIONS

Analytical studies demonstrate that HCHO and CH_3OH in ordinary air can be oxidized by high intensity UV radiation. Oxidation can be achieved also with low-pressure mercury bulbs providing the inlet air is enriched with ozone. A kinetic mechanism is suggested involving direct photolysis and overlapping ozone and HO_2 loops to generate OH which is the primary oxidizing agent. Analytical studies demonstrate that the major portion of photolysis occurs in the boundary layer surrounding a UV bulb and that designers should arrange bulbs in a dense configuration two bulb diameters between centers. Experiments with ethanol in ordinary air demonstrate that oxidation can be achieved providing the radiation contains 185 nm to generate ozone.

While oxidation can be achieved using UV radiation alone, it is unwise to ignore the large oxidation enhancement that can be achieved by titania phototcatalysis (3-8). It is suggested that designers should,

- maximize the ratio of titania surface area to reactor volume,
- minimize the distance between bulbs and titania surfaces,
- minimize reactor pressure drop by using streamlined bulb and titania surfaces or arrange titania surfaces parallel to the direction of flow.

ACKNOWLEDGMENTS

Support for this research was provided in part by a grant from the Air Emissions Reduction Center, New Jersey Institute of Technology and in part by Project 33, Strategic Environmental Research and Development Program (SERDP).

REFERENCES

1. Lewis N. M. and Gatchett A. M., "US. Environmental Protection Agency's SITE Emerging Technology Program: 1991 Update", J. Air & Waste Manage. Assoc., Vol. 41, No 12, p.p. 1645-1653, 1991

2. Lewis N. M., Barkley N. P. and Williams T., "1992 Update of US. EPA's Superfund Innovative Technology Evaluation (SITE) Emerging Technology Program", J. Air & Waste Manage. Assoc., Vol. 42, No 12, p.p. 1644-1656, 1992

3. Prairie M. R., Evans L. R., Stange B. M. and Marinez S. L., "An Investigation of TIO_2 Photocatalysis for the Treatment of Water Contaminated with Metals and Organic Chemicals", Enviro. Sci. Technol., Vol. 27, No 9, pp 1776-1782, 1993

4. Mills G. and Hoffmann M. R. , "Photocatalytic Degradation of Pentachlorophenol on TIO_2 Particles: Identification of Intermediates and Mechanism of Reaction", Enviro. Sci. Technol., Vol. 27, No 8, p.p. 1681-1689, 1993

5. Dibble L. and Raupp G. B., "Fluidized-Bed Photocatalytic Oxidation of Trichloroethylene in Contaminated Airstreams", Enviro. Sci. Technol. Vol. 26, No 3, p.p. 492-495, 1992

6. Kuhler R. J., Santo G. A., Caudill T. R., Betterton E. A. and Arnold R. G., "Photoreductive Dehalogenation of Bromoform with Titanium Dioxide-Cobalt Macrocycle Hybrid Catalysts", Environ. Sci. Technol. Vol. 27, No 10, p.p. 2104-2111, 1993

7. Ninios M. R., Jacoby W. A., Blake D. M. and Milne T. A., "Direct Mass Spectrometric Studies of the Destruction of Hazardous Wastes. 2. Gas-Phase Photocatalytic Oxidation of Trichloroethylene over TIO_2 : Products and Mechanism", Environ. Sci. Technol. Vol. 27, No 4, p.p. 732-740, 1993

8. Kutsuna S., Ebihara Y., Nakamura K. and Ibusuki T., "Heterogeneous Photochemical Reactions Between Volatile Chlorinated Hydrocarbons (Trichloroethene and Tetrachloroethene) And Titanium Dioxide", Atmospheric Environment Vol. 27A, No 4, p.p. 599-604, 1993

9. Martinez R. D., Buitrago A. A., Howell N. W., Hearn C. H. and Joens J. A., "The Near UV Absorption Spectra of Several Aliphatic Aldehydes and Ketones at 300 K", Atmospheric Environment Vol. 26A, No 5, p.p. 785-792, 1992

10. Johnson M. D., Haag W., Blystone P. G. and Daley P. F., "Destruction of Organic Contaminants in Air Using Advanced Ultraviolet Flashlamps", EPA Draft report, Contract CR 818209-01-0, Emerging Technology Section, SDEB, Risk Reduction Engineering Laboratory, Cincinnati, OH, July 1992

11. Anastisi C., Gladstone R. V. and Sanderson M. G., Chemical Amplifiers for Detection of Peroxy Radicals in the Atmosphere", Environ. Sci. Technol. Vol. 27, No 3, p.p. 474-482, 1993

12. Finlayson-Pitts B. J. and Pitts J. N. Jr., "Atmospheric Chemistry of Tropospheric Ozone Formation: Scientific and Regulatory Implications", J. Air & Waste Manage., Vol. 43, p 1091-1100, 1993

13. McRae G. J., Goodin W. R. and Seinfeld J. H., "Development of a Second-Generation Mathematical Model for Urban Air Pollution - I. Model Formulation", Atmospheric Environment, Vol. 16, No 4, p.p. 679-696, 1982

14. McRae G. J. and Seinfeld J. H., "Development of a Second -Generation Mathematical Model for Urban Air Pollution - II. Evaluation of Model Performance", Atmospheric Environment, Vol. 17, No 3, p.p. 501-522, 1983

15. Atkinson R., "Gas-Phase Tropospheric Chemistry of Organic Compounds: A Review", Atmospheric Environment, Vol. 24A, No 1, p.p. 1-41, 1990

16. Atkinson R., Baulich D. L., Cox R. A., Hampson R. F. Jr., Kerr J. A. and Troe J., "Evaluated Kinetic and Photochemical Data for Atmospheric Chemistry: Supplement IV", Atmospheric Environment, Vol. 25A, No 7, p.p. 1187-1230, 1992

17. Fálls A. H. and Seinfeld J. H., "Continued Development of a Kinetic Mechanism for Photochemical Smog", Environ. Sci. & Technol., Vol. 12, No 13, p.p. 1398-1406, 1978

18. Heicklen J., "Atmospheric Chemistry", Academic Press, New York, NY, 1976

19. Seinfeld J. H., "Atmospheric Chemistry and Physics of Air Pollution", Wiley-interscience, New York, NY, 1986

20. Finlayson-Pitts B. J. and Pitts J. N. Jr., "Atmospheric Chemistry: Fundamentals and Experimental Techniques", Wiley-Interscience, New York, NY, 1986

21. Calvert J. G. and Pitts J. N., "Photochemistry", John Wiley & Sons, Inc., New York, 1967

22. Johnson H. S., Page M., and Yao F., "Oxygen Absorption Cross-section in the Herzberg Continuum Between 206 & 327 K", J. Geophysics. Res., Vol. 89, p.p. 11661-11665, 1984

23. DeMore W. B., et. al, "Chemical Kinetics and Photochemical Data for Use in Stratospheric Modeling", Eval #9, NASA, 1 Jan 1990

24. Stockwell W. R. and Calvert J. G., "The Near Ultraviolet Absorption Spectrum of Gaseous HONO and $N_2 O_3$ ", Journal of Photochemistry, Vol. 8, p.p. 193-208, 1978

25. Atkinson R., Blauch D. L., Cox R. A. Jr., Kerr J. A. and Troe J, "Evaluated Kinetic and Photochemical Data for Atmospheric Chemistry", J. Phys. Chem. Ref. Data, Vol. 23, p.p. 1259, 1984

26. Atkinson R., Blauch D. L., Cox R. A. Jr., Kerr J. A. and Troe J. "Evaluated Kinetic and Photochemical Data for Atmospheric Chemistry", J. Phys. Chem. Ref. Data, Vol. 18, p 881, 1989

27. Atkinson R., Blauch D. L., Cox R. A. Jr., Kerr J. A. and Troe J., "Evaluated Kinetic and Photochemical Data for Atmospheric Chemistry", J. Phys. Chem. Ref. Data, Vol. 21, p 1, 1992

28. Witten G. Z., Hogo H. and Killus J. P., "The Carbon-Bond Mechanism: A Condensed Kinetic Mechanism for Photochemical Smog", Enviro. Sci. & Technol., Vol. 14, No 6, p.p. 690-700, 1980

29. Hertel O, Berkowicz R., Christensen J. and Hov O., "Test of Two Numerical Schemes For Use In Atmospheric Transport-Chemistry Models", Atmospheric Environment, Vol. 27A, No 16, pp. 2591-2611, 1993

30. Hess G. D., Carnovale F., Cope M. E. and Johnson G. M., "The Evaluation of Some Photochemical Smog Reaction Mechanisms - I. Temperature and Initial Composition Effects, - II. Initial Addition of Alkanes and Alkenes, - III. Dilution and Emissions Effects", Atmospheric Environment, Vol. 26A, No 4, p.p. 625-659, 1992

31. Creare Inc., "Fluent Manual", Hanover, NH

TABLE I - UV RADIATION SOURCES AND INITIAL GAS COMPOSITION

UV Sources

Case	$[O_3]_0$ (PPM)	UV	λ(nm)	P_λ/A (w/m^2)	J(photons/cm^2 s)
1	0.01	(a)	185	1.99×10^{-4}	1.85×10^{14}
		(a)	253.7	9.93×10^{-3}	1.14×10^{16}
		(b)	337	3.72×10^{-6}	1.45×10^{16}
2	1000	Same as Case 1			
3	0.01	(c)	193	31.4	3.1×10^{19}
4	0.01	(d)	248	25.7	3.21×10^{19}
5	0.01	(e)	308	15.5	2.21×10^{19}

(a) 40-W, low-pressure mercury lamp, 40% overall efficiency; radiant power, 5% 185 nm, 95% 253.7 nm
(b) 0.006 W, N_2 -laser
(c) 55-W, Excimer Ar-F laser
(d) 45-W, Excimer Kr-F laser
(e) 25-W, Excimer Xe-Cl laser

Initial Concentrations

Cases 1,3,4,5: Ordinary ambient air containing 1000 PPM of HCHO and CH_3OH

$[O_3]_0 = 0.01$ PPM
$[H_2O_2]_0 = 0.01$ PPM
$[OH]_0 = 4.1\times10^{-9}$ PPM
$[HO_2]_0 = 4.1\times10^{-6}$ PPM
$[CO_2]_0 = 300$ PPM
$[O(^3P)]_0 = 1.2\times10^{-11}$ PPM
$[H_2O]_0 = 22{,}500$ PPM (70% RH)
$[NO]_0 = 0.01$ PPM
$[NO_2]_0 = 0.1$ PPM
$[CO]_0 = 0.1$ PPM
$[O(^1D)]_0 = 8.1\times10^{-13}$ PPM
$[\text{all other species}]_0 = 0$

Case 2: Ozonated Air, same as Case 1 above except $[O_3]_0 = 1000$ PPM

TABLE II - RADICAL REACTIONS AND RATE CONSTANTS

Reaction & Number		Rate constant ($cm^3 molecule^{-1} s^{-1}$)
$OH + O_3 = HO_2 + O_2$	(R1)	6.7E-14
$HO_2 + O_3 = OH + 2O_2$	(R2)	2.0E-15
$NO + O_3 = NO_2 + O_2$	(R3)	1.8E-14
$NO_2 + O_3 = NO_3 + O_2$	(R4)	1.2E-13
$HCO + O_2 = HO_2 + CO$	(R9)	5.6E-12
$HCHO + OH = CO + H_2O$	(R10)	1.1E-11
$OH + OH = H_2O + O(^1D)$	(R11)	1.9E-12
$OH + HO_2 = H_2O + O_2$	(R12)	1.1E-10
$OH + H_2O_2 = H_2O + HO_2$	(R13)	1.7E-12
$NO_2 + OH = HNO_3$	(R14)	1.1E-11
$CO + OH = CO_2 + H$	(R15)	2.9E-13
$N + OH = NO + H$	(R16)	4.9E-11
$HCHO + OH = H_2O + HCO$	(R17)	1.0E-11
$H + O_2 = HO_2$	(R18)	1.2E-12
$H + O_3 = OH + O_2$	(R19)	2.9E-11
$HO_2 + HO_2 = H_2O_2 + O_2$	(R20)	1.6E-12
$NO + HO_2 = NO_2 + OH$	(R22)	8.3E-12
$NO_2 + HO_2 = HONO + O_2$	(R23)	1.4E-14
$CO + HO_2 = CO_2 + OH$	(R24)	1.9E-32
$O(^1D) + N_2 = O(^3P) + N_2$	(R30)	1.8E-11
$O(^3P) + O_2 + M = O_3 + M$	(R31)	2.9E-11
$NO + O(^3P) + M = NO_2 + M$	(R32)	3.0E-11
$NO_2 + O(^3P) = O_2 + NO$	(R33)	9.7E-12
$O(^3P) + O_3 = O_2 + O_2$	(R35)	9.5E-15
$O(^1D) + H_2O = OH + OH$	(R36)	2.2E-10
$O(^1D) + O_3 = O_2 + O(^3P) + O(^3P)$	(R37)	1.2E-11
$O(^1D) + O_2 = O(^3P) + O_2$	(R38)	4.0E-11
$NO + OH = HONO$	(R51)	1.1E-11
$HONO + OH = H_2O + NO_2$	(R52)	4.9E-12
$CH_3OH + OH = 0.85CH_2OH + 0.15\{CH_3O + H_2O\}$	(R60)	7.8E-13
$CH_2OH + O_2 = HCHO + HO_2$	(R61)	9.8E-12
$CH_3 + O_2 = HCHO + HO_2$	(R62)	1.9E-15

TABLE III - PHOTOLYTIC RATE CONSTANTS (s^{-1})

Reaction	No	Cases 1 & 2	Case 3	Case 4	Case 5
$HCHO + h\nu \rightarrow H + HCO$	(P1A)	1.30E-5	0	1.63E-2	7.76E-1
$HCHO + h\nu \rightarrow H + HCO$	(P1B)	3.86E-5	0	2.86E-2	2.19E-1
$CH_3OH + h\nu \rightarrow$	(P2)	negligible			
$O_3 + h\nu \rightarrow O(^1D) + O_2$	(P3A)	1.12E-1	1.38E1	3.27E2	3.04E0
$O_3 + h\nu \rightarrow O(^3P) + O_2$	(P3B)	1.32E-2	0	3.63E1	0
$O_2 + h\nu \rightarrow O(^1D) + O(^3P)$	(P4A)	0	0	0	0
$O_2 + h\nu \rightarrow O(^3P) + O(^3P)$	(P4B)	1.23E-30	2.75E-4	0	0
$O_2 + h\nu \rightarrow O(^1D) + O(^1D)$	(P4C)	0	0	0	0
$H_2O_2 + h\nu \rightarrow OH + OH$	(P5A)	8.52E-4	1.85E1	2.91E0	9.68E-2
$H_2O_2 + h\nu \rightarrow H_2O + O(^1D)$	(P5B)	0	0	0	0
$H_2O_2 + h\nu \rightarrow H + HO_2$	(P5C)	0	0	0	0
$H_2O_2 + h\nu \rightarrow 2H + O_2$	(P5D)	0	0	0	0
$NO_2 + h\nu \rightarrow NO + O(^1D)$	(P6A)	0	0	0	0
$NO_2 + h\nu \rightarrow NO + O(^3P)$	(P6B)	7.42E-4	0	6.94E-1	3.58E0
$H_2O + h\nu \rightarrow H_2 + O(^3P)$	(P7A)	0	0	0	0
$H_2O + h\nu \rightarrow H + OH$	(P7B)	1.09E-5	0	0	0
$H_2O + h\nu \rightarrow H_2 + O(^1D)$	(P7C)	0	0	0	0
$HONO + h\nu \rightarrow NO + OH$	(P50A)	2.61E-3	4.70E1	4.77E1	1.07E-1
$HONO + h\nu \rightarrow H + NO_2$	(P50B)	0	0	0	0
$HONO + h\nu \rightarrow HNO + O(^3P)$	(P50C)	0	0	0	0
$CO_2 + h\nu \rightarrow CO + O(^1D)$	negligible				
$CO_2 + h\nu \rightarrow CO + O(^3P)$	negligible				

Actinic Flux (photons/cm^2 /s)

Case 1 and 2, $J(185\ nm) = 1.85 \times 10^{14}$
$J(253.7\ nm) = 1.14 \times 10^{16}$
$J(337\ nm) = 1.45 \times 10^{16}$

Case 3, $J(193\ nm) = 3.1 \times 10^{19}$

Case 4, $J(248\ nm) = 3.21 \times 10^{19}$

Case 5, $J(308\ nm) = 2.21 \times 10^{19}$

TABLE OF FIGURE AND TABLE CAPTIONS

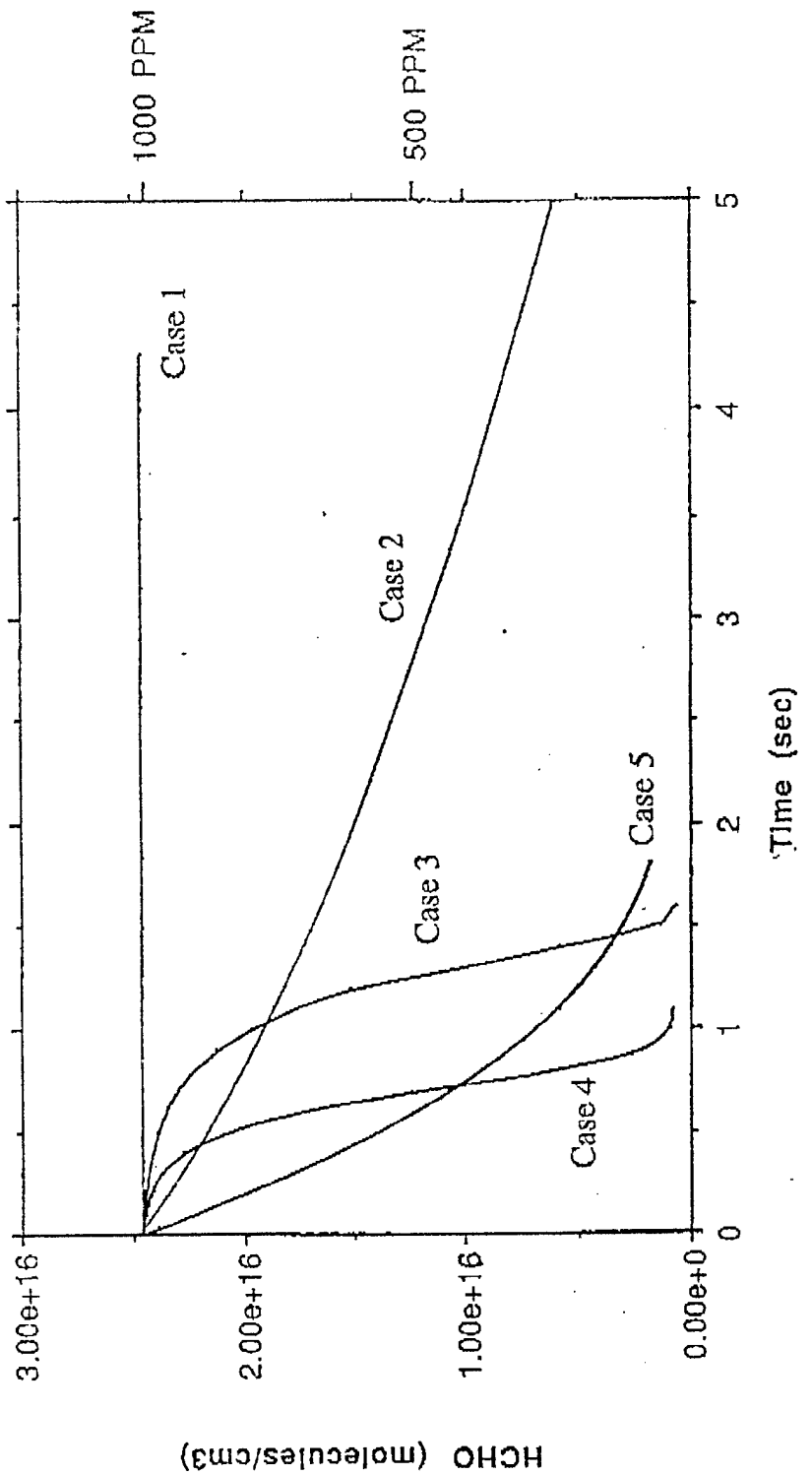

Figure 1 - Predicted HCHO concentration versus time for five different UV irradiations

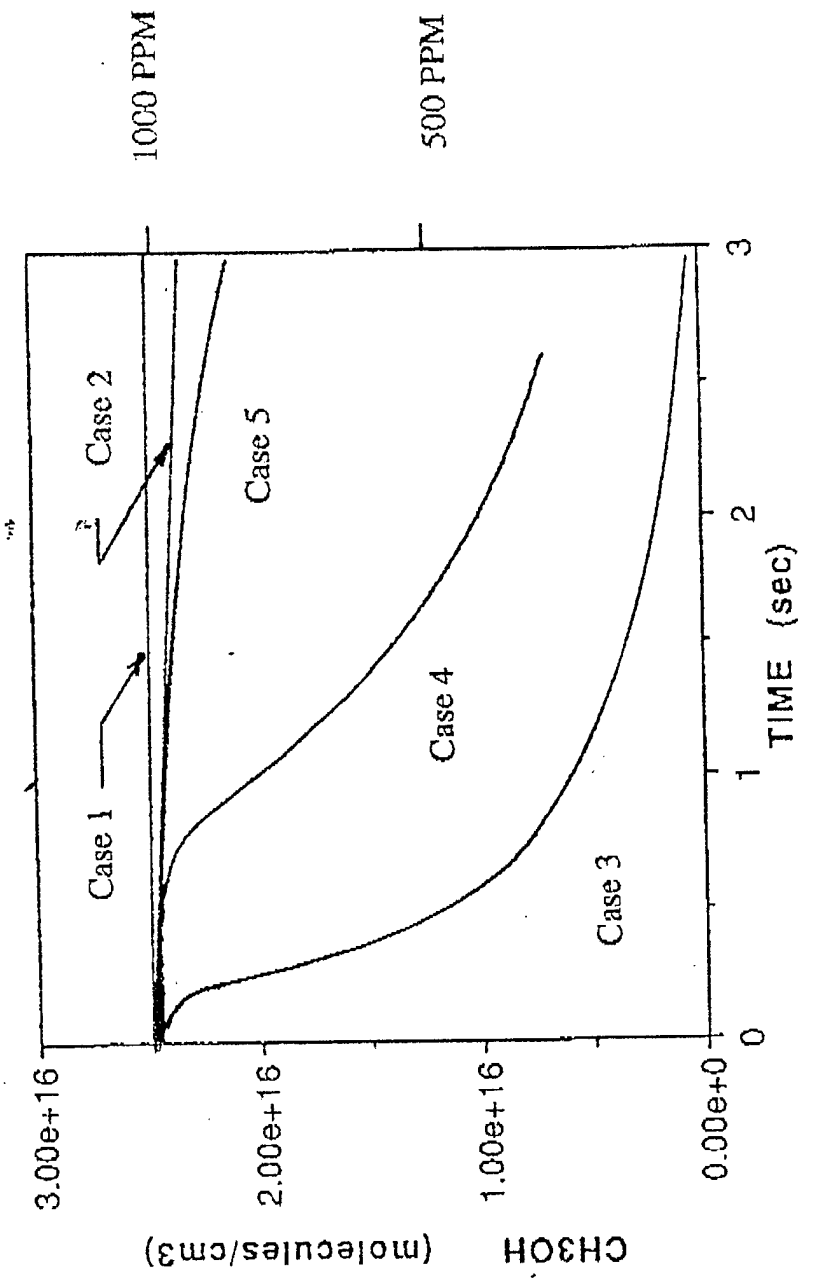

Figure 2 - Predicted CH_3OH concentration versus time for five different UV irradiations

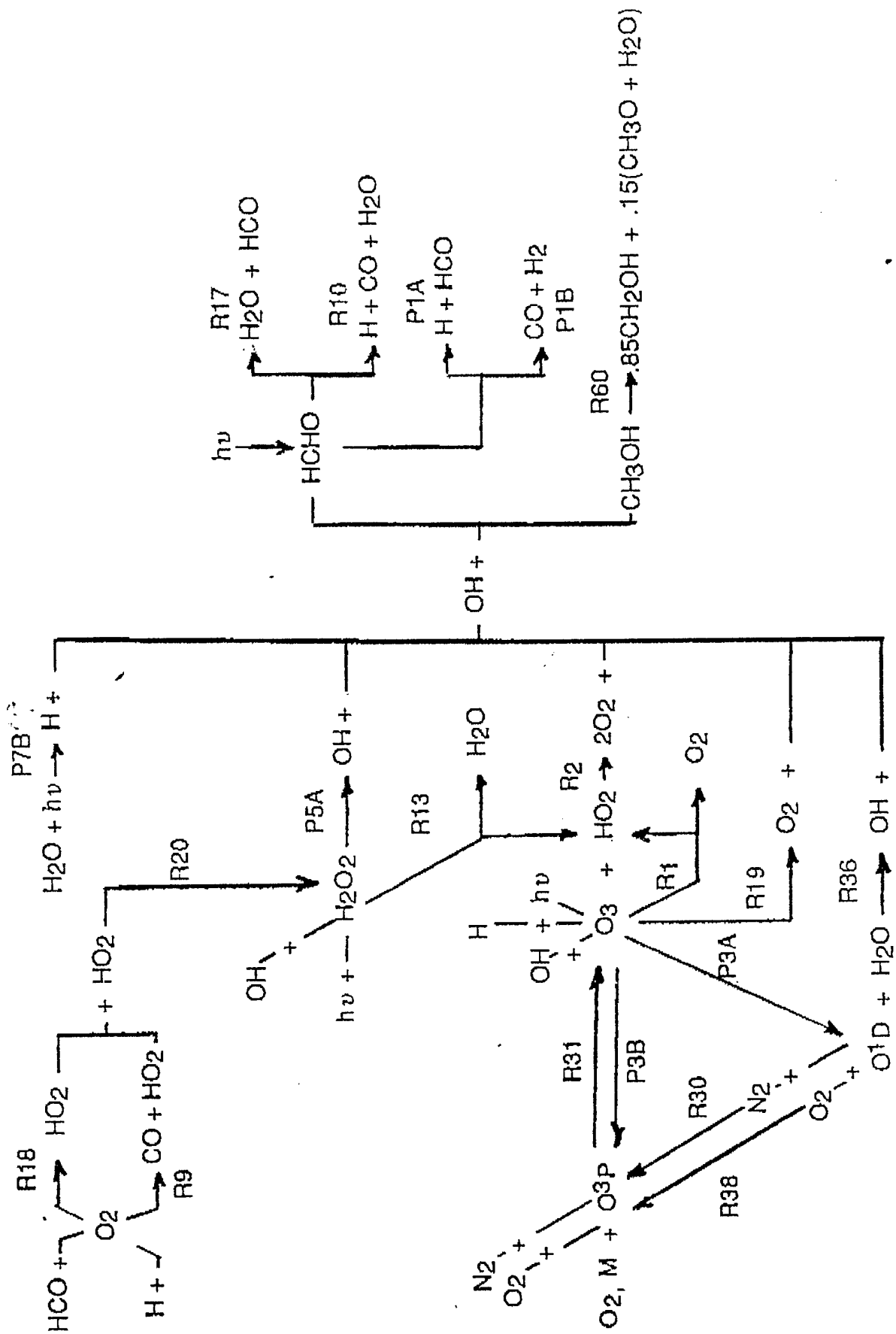

Figure 3 - Schematic diagram of the simplified UV radical oxidation mechanism for HCHO and CH_3OH in ordinary air

HCHO

$$\frac{d[HCHO]}{dt} = -(K17+K10)-(P1A+P1B)+R61-R62$$

$$=(K17+K10)[HCHO][OH]-(KP1A+KP1B)[HCHO]$$

$$=K61[CH_2OH][O_2]+K62[CH_3O][O_2]$$

OH

$$\frac{d[OH]}{dt} = R2-R10-R17-R13+R19+R36-R12$$

$$-R15-R60+P7B+P5A-R1$$

$$K2[HO_2][O_3]-K10[HCHO][OH]-K17[HCHO][OH]$$

$$-K13[H_2O_2][OH]+K19[H][O_3]+2K36[O(^1D)][H_2O]$$

$$-K12[OH][HO_2]-K15[CO][OH]-K60[CH_3OH][OH]$$

$$+KP7B[H_2O]+KP5A[H_2O_2]-K1[OH][O_3]$$

H

$$\frac{d[H]}{dt} = P7B+R10-R16+R15-R19$$

$$KP7B[H_2O]+K10[HCHO][OH]-K16[H][O_2]+K15[CO][OH]$$

$$-K19[H][O_3]$$

HO_2

$$\frac{d[HO_2]}{dt} = R16+R9-R20+R13+R1-R2$$

$$=[O_2]\{K16[H]+K9[HCO]\}-K20[HO_2]^2+K13[OH][H_2O_2]$$

$$+K2[OH][O_3]-K2[HO_2][O_3]$$

$O(^3P)$

$$\frac{d[O(^3P)]}{dt} = R30-R31+P3B+R38$$

$$KP3B[O_3]+R30[O(^1D)][N_2]-R31[O(^3P)][O_2]+R38[O(^1D)][O_2]$$

$O(^1D)$

$$\frac{d[O(^1D)]}{dt} = P3A-R30-R36-R38$$

$$=KP3A[O_3]-[O(^1D)]\{K30[N_2]+K36[H_2O]+K38[O_2]\}$$

H_2O_2

$$\frac{d[H_2O_2]}{dt} = R20-P5A-R13$$

$$=K20[HO_2]^2-KP5A[H_2O_2]-K13[H_2O_2][OH]$$

O_3

$$\frac{d[O_3]}{dt} = R31-P3A-P3B-R2-R19-R1$$

$$=K31[O(^3P)][O_2]-[O_3]\{KP3A+KP3B\}-K2[HO_2][O_3]-K19[H][O_3]$$

$$-K1[OH][O_3]$$

HCO

$$\frac{d[HCO]}{dt} = P1A+R17-R9$$

$$=KP1A[HCHO]+K17[HCHO][OH]-K9[HCO][O_2]$$

Figure 4 - Ordinary differential equations for the simplified UV radical oxidation mechanism for HCHO and CH_3OH in ordinary air

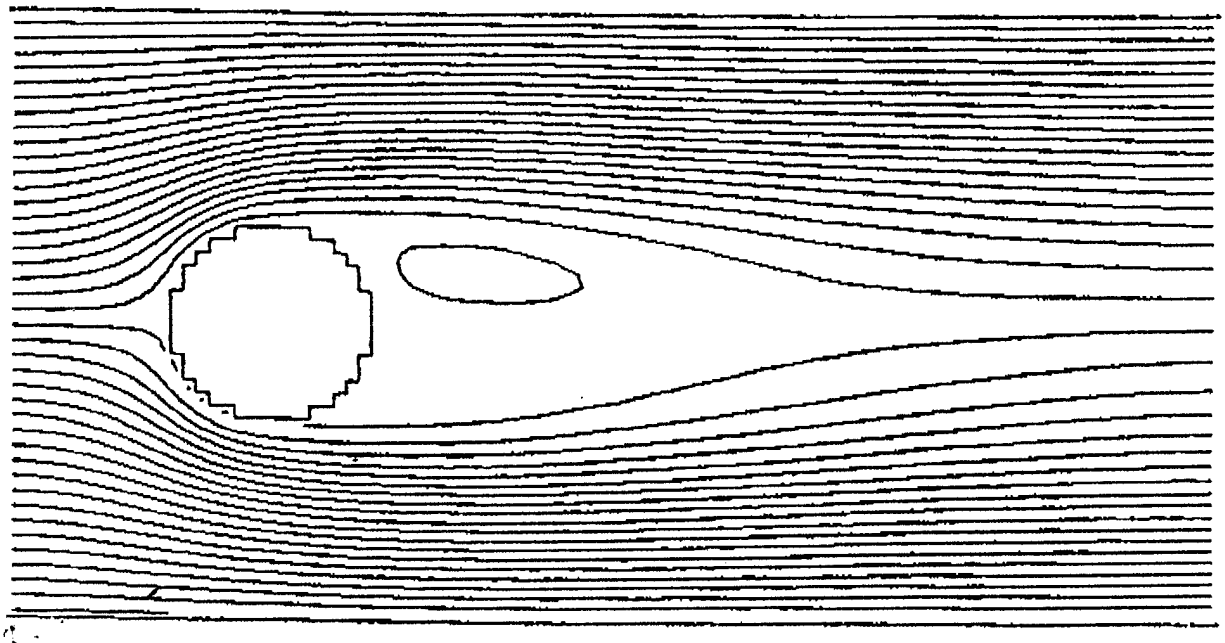

Figure 5 - Wake region of UV bulb in uniform flow,
gas velocity = 2 m/s, bulb diameter = 0.03 m

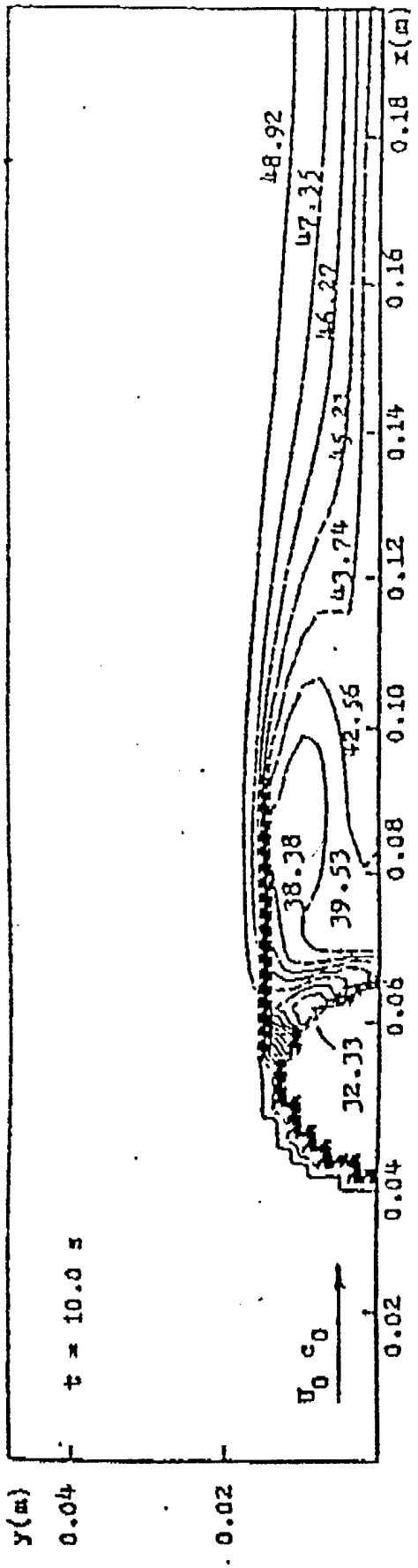

Figure 6 - Predicted HCHO concentrations in vicinity of UV bulb, gas velocity = 2 m/s, bulb diameter = 0.03 m, $[HCHO]_0$ = 50 PPM

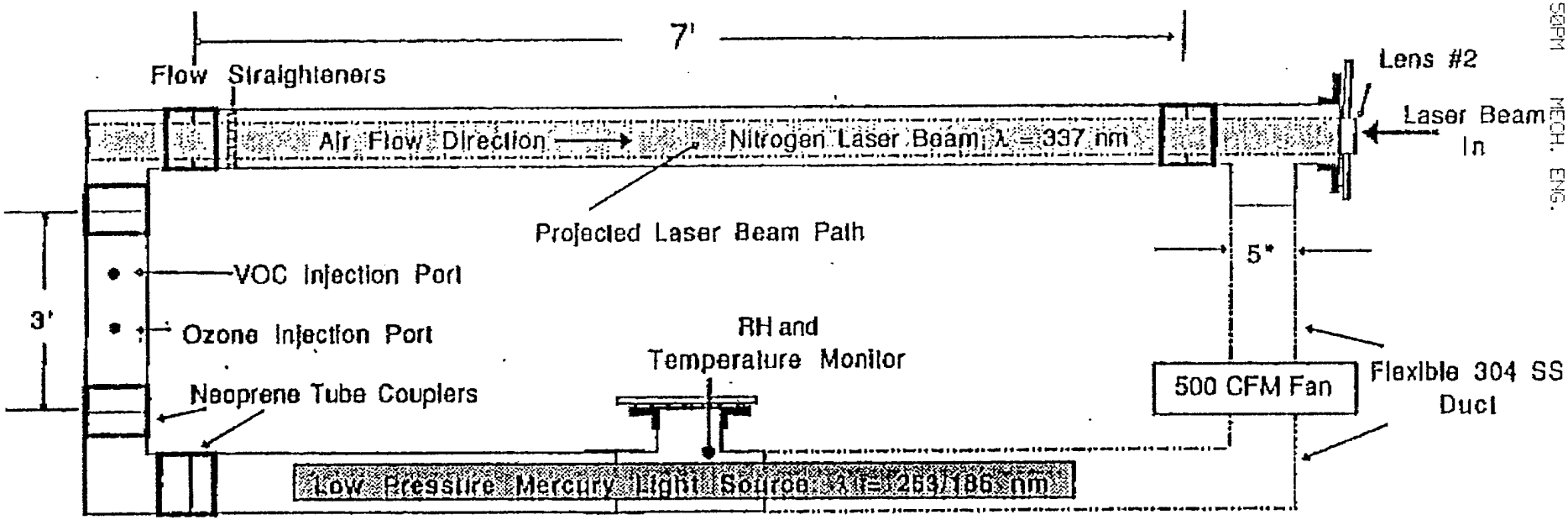

Figure 7 - Steady flow, closed loop experimental photolytic reactor

AUG.22.1997 3:50PM MECH. ENG. NO.960 P.24

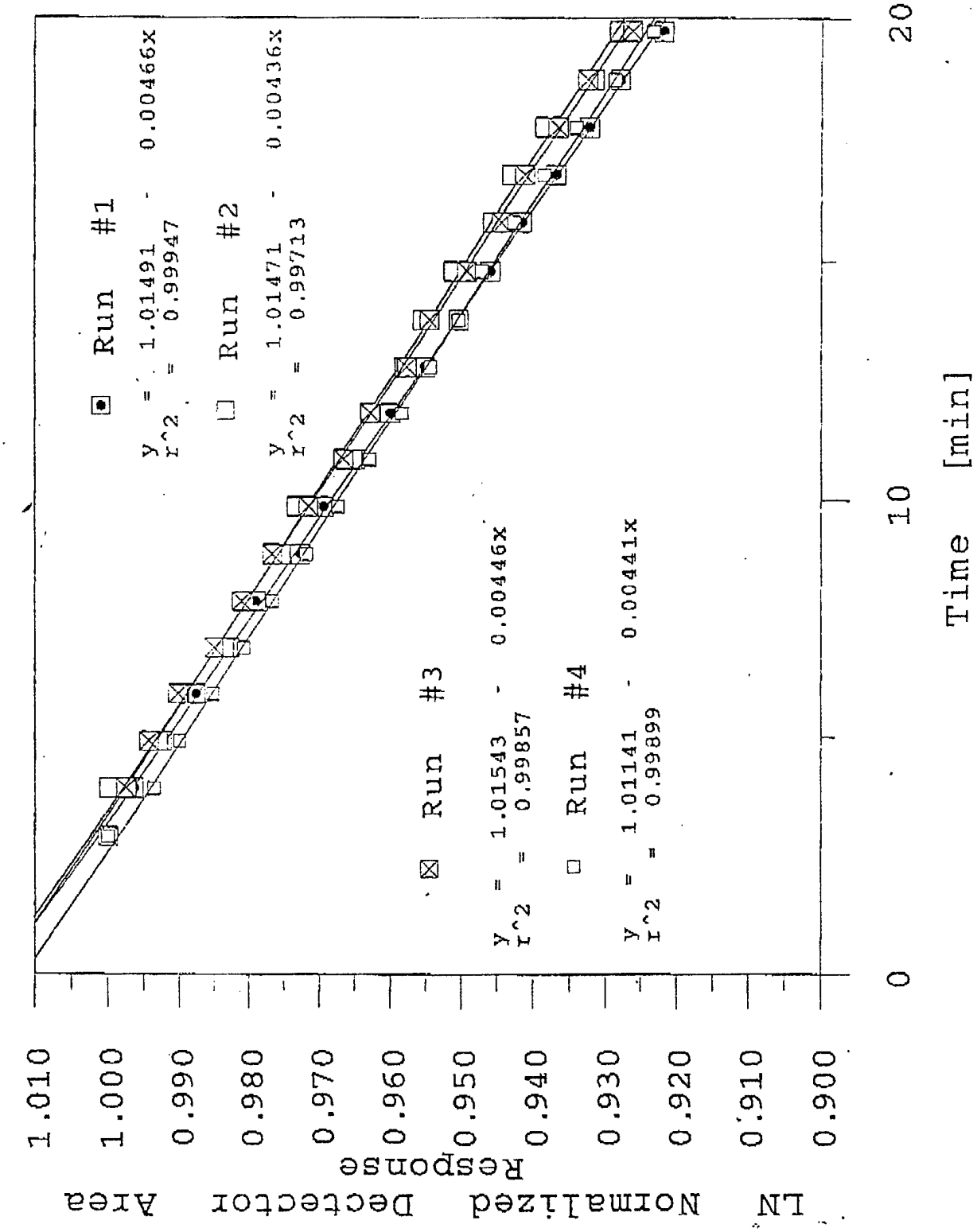

Figure 8 - Natural logarithm of ethanol area response versus time for ethanol vapor in air irradiated by three, low-pressure mercury lamps